

Three-loop four-particle QCD amplitudes

Piotr Bargieła^{a,*}

^a*Rudolf Peierls Centre for Theoretical Physics, University of Oxford,
Clarendon Laboratory, Parks Road, Oxford OX1 3PU, U.K.*

E-mail: piotr.bargiela@physics.ox.ac.uk

We present recent advancements in the computation of three-loop four-particle helicity amplitudes in full-color massless QCD. In this contribution, we focus on the $gg \rightarrow \gamma\gamma$ process. We show how to obtain compact analytic formulae for the three-loop scattering amplitude. Our results can be expressed in terms of harmonic polylogarithms, which allows for an efficient numerical evaluation. The results presented here can be used for improving theoretical predictions relevant for Higgs physics at hadron colliders.

*41st International Conference on High Energy physics - ICHEP2022
6-13 July, 2022
Bologna, Italy*

*Speaker

1. Introduction

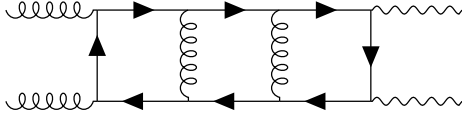
This year, we are celebrating the 10th anniversary of the Higgs boson discovery at the Large Hadron Collider (LHC) [1, 2]. With this achievement, the particle content of the Standard Model has been confirmed. Nonetheless, further efforts are still necessary in order to well establish all properties of fundamental interactions. Experimentally, it requires performing high-precision measurements of physical observables. Theoretically, this precision needs to be matched by Standard Model predictions. At the LHC, most of the real and virtual radiation is due to strong interactions, described by Quantum Chromodynamics (QCD). Accurate theoretical predictions require higher-order perturbative calculations. For virtual corrections, this in turn requires the knowledge of multi-loop scattering amplitudes. Only recently, the three-loop precision has been reached in the full-color QCD for the following processes: $q\bar{q} \rightarrow \gamma\gamma$ [3], $q\bar{q} \rightarrow q\bar{q}$ [4], $gg \rightarrow \gamma\gamma$ [5], $gg \rightarrow gg$ [6], $q\bar{q} \rightarrow gg$ [7] (listed here chronologically). Here we will focus on the computation of the amplitude for $gg \rightarrow \gamma\gamma$ [5].

2. Computation

Let us consider the three-loop amplitude for the $g(p_1) + g(p_2) \rightarrow \gamma(-p_3) + \gamma(-p_4)$ process. At this order, there are 3299 Feynman diagrams, one of which is depicted in Fig. 1. This number is almost 24 times larger than at the two-loop level, but still about 15 times smaller than for the $gg \rightarrow gg$ process. When all Feynman diagrams are summed up to obtain the three-loop amplitude, the result contains three structures: color, Lorentz tensors, and Feynman integrals. The color structure can be extracted either formally, following $SU(3)$ Lie algebra, or diagrammatically, using 't Hooft's double line formalism [8]. For this process, the color algebra does not pose any challenge. In particular, color factors can be expressed in terms of quadratic Casimir invariants. Therefore, from now on we will focus on the much more involved tensor and integral structures.

Before computing the required Feynman integrals, we transformed the integrand into a Lorentz scalar form. In general, there are non-trivial Lorentz vector indices arising from external polarization vectors and γ matrices originating from the $\bar{q}\gamma^\mu q$ vertex structures. Given the large number of Feynman diagrams involved, these quickly lead to a lot of different Lorentz tensor structures. From now on, we will refer to these structures simply as *tensors*. If one were to enumerate the independent tensors in d dimensions for this process at three loops, they would find 138 inequivalent ones. This number can be reduced to 10 by requiring transversality and by choosing an explicit reference vector for the external polarisation vectors. On the other hand, the number of independent helicity states in $d=4$ is $2^4/2=8$, assuming parity invariance. Therefore, the number of 10 tensors independent in d dimensions should be possible to further reduce to 8 in four dimensions. This is indeed possible [9, 10]. In particular, if one works in the 't Hooft-Veltman scheme, one can project out two redundant tensors from the four-dimensional subspace with a standard orthogonalization procedure and only deal with 8 independent structures. This approach is loop-universal and it provides a 1-to-1 correspondence between helicity amplitudes and Lorentz scalar coefficients in the tensor basis, called *form factors*.

After expressing the amplitude in terms of form factors, one is left with a large number of three-loop Feynman integrals to evaluate. In our case, we obtained about $4 \cdot 10^6$ different Feynman



$$\begin{aligned}
 &= g_s^6 e^2 n_f^{(V_2)} C_f^2 \delta^{a_1, a_2} \int \frac{d^d k_1}{(2\pi)^d} \frac{d^d k_2}{(2\pi)^d} \frac{d^d k_3}{(2\pi)^d} \\
 &\times \frac{\text{tr} [\not{\epsilon}_1(\not{k}_1)\not{\epsilon}_2(\not{k}_1 + \not{p}_2)\gamma^\mu(\not{k}_{13} + \not{p}_2)\gamma^\nu(\not{k}_2 + \not{p}_4)\not{\epsilon}_4(\not{k}_2)\not{\epsilon}_3(\not{k}_2 - \not{p}_3)\gamma_\nu(\not{k}_{13} - \not{p}_1)\gamma_\mu(\not{k}_1 - \not{p}_1)]}{(k_1)^2(k_1 + p_2)^2(k_{13} + p_2)^2(k_2 + p_4)^2(k_2)^2(k_2 - p_3)^2(k_{13} - p_1)^2(k_1 - p_1)^2(k_3)^2(k_{123} - p_{13})^2}
 \end{aligned}$$

color tensors integrals

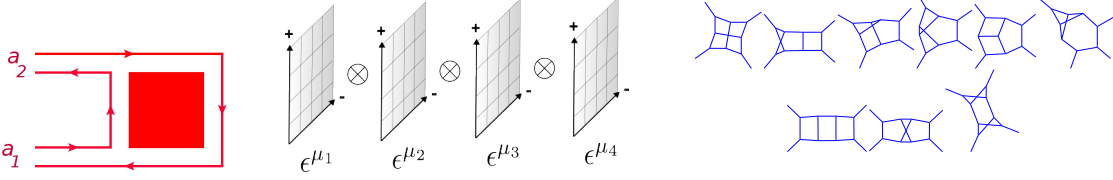


Figure 1: Example Feynman diagram and the three corresponding structures in the amplitude.

integrals. In order to compute them in an efficient way, we reduced them to a minimal basis, and then evaluated only this set. They reduced the number of integrals by $\mathcal{O}(20)$. The most involved step was to use the Integration-By-Parts (IBP) relations [11] to project all remaining integrals onto a basis set of Master Integrals (MIs). In general, coefficients in the MI basis are rational functions of the dimension d and kinematic invariants. IBP identities follow from the shift invariance of scalar Feynman integrals, and together with Lorentz invariance identities generate a linear system [12]. In order to solve such a complicated system, we made use of some modern mathematical methods. We exploited \mathbb{F}_p finite-field arithmetic [13] to numerically reconstruct analytic expressions for the rational coefficient functions. In addition, we used syzygy-based techniques [14] from algebraic geometry to constrain the number of redundant integrals generated by IBP relations. Moreover, we partial fractioned the rational coefficient functions in both the dimension d and kinematic invariants. It exposed the analytic structure of the amplitude, which consists of poles and branch cuts in the kinematic invariants coming from the rational functions and MIs. In this manner, we obtained a fully analytic decomposition of all $4 \cdot 10^6$ integrals in a basis of 486 MIs.

The analytic expressions for four-particle three-loop massless MIs have been computed before [15]. Nonetheless, we have decided to recompute them independently as a check. The modern approach to finding analytic expressions for MIs relies on two steps: constructing a Differential Equation (DE) in the kinematics invariants, and computing the associated boundary condition. Firstly, one can find a set of MIs for each of the 9 integral families depicted in Fig. 1 (bottom-right). Since MIs form a basis, a derivative of a MI can be further IBP reduced in the same basis of MIs, thus closing the system of DEs. With an appropriate choice of MI basis, the DE has a so-called *canonical form* [16], and can be easily solved perturbatively in the dimensional regulator $\epsilon = (4 - d)/2$. At each ϵ^n order, the result can be written in terms of the well-known Harmonic Polylogarithms (HPL) [17] with only two letters, 0 and 1, in correspondence with poles of the DE. Secondly, our general solution to the DE requires fixing the associated boundary condition.

For planar topologies, one could obtain information about the boundary terms by requiring that the solution does not contain a particular branch cut in some physical channel, see e.g. Ref. [18]. Since for the complicated non-planar topologies this method does not work, we relied on the UV regularity constraint [15]. It follows from an assumption that Feynman integrals should be regular around each pole of the DE. The DE can be directly solved in a vicinity of the pole, which generates linear relations between boundary constants. In fact, for our DE, all boundary conditions can be related, order by order in ϵ , to a single overall normalization factor. This is in agreement with Ref. [15]. Therefore, in this manner, we had to compute only one simple overall normalization integral with direct integration methods in order to reconstruct all the $4 \cdot 10^6$ Feynman integrals in the problem.

3. Results

The final expression for the bare scattering amplitude is linear in HPLs with rational function coefficients, expanded as a series in powers of ϵ . Since the UV and IR behaviour is universal, we can predict all ϵ poles from lower-loop results. Due to the Kinoshita-Lee-Nauenberg theorem, these poles cancel exactly against real emission divergences when combining into the partonic cross section. Thus, the genuinely new physical information is contained in the UV-renormalized IR-finite part of the amplitude. Remarkably, huge expressions present at intermediate stages of the calculation can be reduced with aforementioned methods into a compact formula. For the simplest helicity configuration, the finite part of the amplitude reads

$$\begin{aligned}
f_{++++}^{(3,\text{fin})} &= \Delta_1(x) n_f^2 C_A^2 + \Delta_2(x) n_f^2 C_A C_F + \Delta_3(x) n_f n_f^2 C_A + \Delta_4(x) (n_f^V)^2 C_A + \Delta_5(x) n_f^2 C_F^2 + \Delta_6(x) (n_f^V)^2 C_F + \Delta_7(x) n_f n_f^2 C_F + \Delta_8(x) n_f^2 n_f^2 \\
&\quad + \{(x) \leftrightarrow (1-x)\}, \\
\Delta_1(x) &= -\frac{23L_1(L_1+2i\pi)}{9x^2} + \frac{32L_1(L_1+2i\pi) - 46(L_1+i\pi)}{9x} - \frac{17}{36}L_0^2 - \frac{19}{36}L_0L_1 + \frac{1}{9}L_0 - 2i\pi L_0 + \frac{1}{288}\pi^4 \\
&\quad - \frac{373}{72}\zeta_3 - \frac{185}{72}\pi^2 + \frac{4519}{324} + \frac{1}{2}i\pi\zeta_3 + \frac{11}{144}i\pi^3 + \frac{157}{12}i\pi + \frac{43}{9}L_0x - \frac{7}{9}x^2 \left((L_0 - L_1)^2 + \pi^2 \right), \\
\Delta_2(x) &= \frac{8L_1(L_1+2i\pi)}{3x^2} + \frac{16(L_1+i\pi) - 8L_1(L_1+2i\pi)}{3x} - \frac{1}{3}L_0^2 + \frac{5}{6}L_0L_1 + \frac{17}{3}L_0 + i\pi L_0 - \frac{5}{12}\pi^2 - \frac{199}{6} - 8i\pi - \frac{16}{3}L_0x + \frac{4}{3}x^2 \left((L_0 - L_1)^2 + \pi^2 \right), \\
\Delta_3(x) &= \frac{L_1(L_1+2i\pi)}{18x^2} + \frac{2(L_1+i\pi) - L_1(L_1+2i\pi)}{18x} - \frac{1}{36}L_0^2 + \frac{1}{36}L_0L_1 - \frac{1}{9}L_0 - \frac{61}{36}\zeta_3 + \frac{475}{432}\pi^2 - \frac{925}{324} - \frac{1}{72}i\pi^3 - \frac{175}{54}i\pi + \frac{2}{9}L_0x + \frac{1}{36}x^2 \left((L_0 - L_1)^2 + \pi^2 \right), \\
\Delta_4(x) &= -\frac{5L_1(L_1+2i\pi)}{4x^2} + \frac{L_1(L_1+2i\pi) - 8(L_1+i\pi)}{2x} + \frac{1}{4}L_0^2 - \frac{1}{4}L_0L_1 - 2L_0 - 6\zeta_3 + \frac{1}{8}\pi^2 - \frac{1}{2} + 4L_0x - x^2 \left((L_0 - L_1)^2 + \pi^2 \right), \\
\Delta_5(x) &= -\frac{L_1(L_1+2i\pi)}{x^2} + \frac{L_1(L_1+2i\pi) - 2(L_1+i\pi)}{x} - \frac{1}{2}L_0^2 - i\pi L_0 + \frac{39}{4} + i\pi + 2L_0x - \frac{1}{2}x^2 \left((L_0 - L_1)^2 + \pi^2 \right), \\
\Delta_6(x) &= \frac{10L_1(L_1+2i\pi)}{3x^2} + \frac{32(L_1+i\pi) - 4L_1(L_1+2i\pi)}{3x} - \frac{2}{3}L_0^2 + \frac{2}{3}L_0L_1 + \frac{16}{3}L_0 + 16\zeta_3 - \frac{1}{3}\pi^2 + \frac{4}{3} - \frac{32}{3}L_0x + \frac{8}{3}x^2 \left((L_0 - L_1)^2 + \pi^2 \right), \\
\Delta_7(x) &= \frac{5L_1(L_1+2i\pi)}{3x^2} + \frac{10(L_1+i\pi) - 8L_1(L_1+2i\pi)}{3x} + \frac{2}{3}L_0^2 + \frac{1}{3}L_0L_1 - \frac{10}{3}L_0 + 2i\pi L_0 + 4\zeta_3 - \frac{\pi^2}{6} + 5 - 3i\pi - \frac{10}{3}L_0x + \frac{1}{3}x^2 \left((L_0 - L_1)^2 + \pi^2 \right), \\
\Delta_8(x) &= -\frac{23}{216}\pi^2 + \frac{5}{27}i\pi, \quad \text{where} \quad L_0 = \ln(x), \quad L_1 = \ln(1-x).
\end{aligned}$$

The simplicity of the result partially originates from the lack of tree-level amplitude for this process. Moreover, the all-plus amplitude is just a constant at one-loop order, thus dropping the highest transcendental weight by two. Still, the complexity of amplitudes in other helicity configurations does not increase beyond $O(10)$ with respect to the expression above. After cancelling spurious poles in the kinematic variable $x = -(p_1 + p_3)^2 / (p_1 + p_2)^2$, these compact expressions can be efficiently evaluated numerically in $O(\mu s)$ per each phase-space point.

4. Outlook

Future directions of investigations are twofold, phenomenological and formal. Phenomenologically, the three-loop amplitude for $gg \rightarrow \gamma\gamma$ can be used to compute a fully differential hadronic

cross section. In particular, the three-loop amplitude computed here, together with two-loop results for $\gamma\gamma$ -jet production [19], allow one to compute theoretical predictions for gluon-induced diphoton production at the LHC at next-to-next-to-leading order (NNLO). Although the main diphoton production mechanism at the LHC is through quark annihilation, the gluon fusion channel is interesting because it interferes with the Higgs boson amplitude and such an interference can be used to put bounds on the value of lifetime of the Higgs boson [20, 21]. On the formal side, the described methods can be used for other three-loop four-particle massless processes. Computing three-loop QCD corrections to γ -jet production and light-by-light scattering would complete the set of $2 \rightarrow 2$ massless scattering amplitudes at this perturbative order. In addition, it would be interesting to understand why these processes require only one independent boundary MI. The answer to this question may help us unveil the hidden amplitude structure.

Acknowledgments

PB is thankful to all the authors of three-loop four-particle amplitude publications: Fabrizio Caola, Amlan Chakraborty, Giulio Gambuti, Andreas von Manteuffel, and Lorenzo Tancredi. The research of PB was supported by the ERC Starting Grant 804394 HipQCD. Graphs were drawn with JaxoDraw [22, 23], Qgraf-XML-drawer [24], and Inkscape [25].

References

- [1] ATLAS collaboration, G. Aad et al., *Observation of a new particle in the search for the Standard Model Higgs boson with the ATLAS detector at the LHC*, *Phys. Lett. B* **716** (2012) 1–29, [[1207.7214](#)].
- [2] CMS collaboration, S. Chatrchyan et al., *Observation of a New Boson at a Mass of 125 GeV with the CMS Experiment at the LHC*, *Phys. Lett. B* **716** (2012) 30–61, [[1207.7235](#)].
- [3] F. Caola, A. Von Manteuffel and L. Tancredi, *Diphoton Amplitudes in Three-Loop Quantum Chromodynamics*, *Phys. Rev. Lett.* **126** (2021) 112004, [[2011.13946](#)].
- [4] F. Caola, A. Chakraborty, G. Gambuti, A. von Manteuffel and L. Tancredi, *Three-loop helicity amplitudes for four-quark scattering in massless QCD*, *JHEP* **10** (2021) 206, [[2108.00055](#)].
- [5] P. Bargiela, F. Caola, A. von Manteuffel and L. Tancredi, *Three-loop helicity amplitudes for diphoton production in gluon fusion*, *JHEP* **02** (2022) 153, [[2111.13595](#)].
- [6] F. Caola, A. Chakraborty, G. Gambuti, A. von Manteuffel and L. Tancredi, *Three-Loop Gluon Scattering in QCD and the Gluon Regge Trajectory*, *Phys. Rev. Lett.* **128** (2022) 212001, [[2112.11097](#)].
- [7] F. Caola, A. Chakraborty, G. Gambuti, A. von Manteuffel and L. Tancredi, *Three-loop helicity amplitudes for quark-gluon scattering in QCD*, [2207.03503](#).
- [8] G. 't Hooft, *A Planar Diagram Theory for Strong Interactions*, *Nucl. Phys. B* **72** (1974) 461.

- [9] T. Peraro and L. Tancredi, *Physical projectors for multi-leg helicity amplitudes*, *JHEP* **07** (2019) 114, [[1906.03298](#)].
- [10] T. Peraro and L. Tancredi, *Tensor decomposition for bosonic and fermionic scattering amplitudes*, *Phys. Rev. D* **103** (2021) 054042, [[2012.00820](#)].
- [11] K. G. Chetyrkin and F. V. Tkachov, *Integration by Parts: The Algorithm to Calculate beta Functions in 4 Loops*, *Nucl. Phys. B* **192** (1981) 159–204.
- [12] S. Laporta, *High precision calculation of multiloop Feynman integrals by difference equations*, *Int. J. Mod. Phys. A* **15** (2000) 5087–5159, [[hep-ph/0102033](#)].
- [13] A. von Manteuffel and R. M. Schabinger, *A novel approach to integration by parts reduction*, *Phys. Lett. B* **744** (2015) 101–104, [[1406.4513](#)].
- [14] J. Gluza, K. Kajda and D. A. Kosower, *Towards a Basis for Planar Two-Loop Integrals*, *Phys. Rev. D* **83** (2011) 045012, [[1009.0472](#)].
- [15] J. Henn, B. Mistlberger, V. A. Smirnov and P. Wasser, *Constructing d -log integrands and computing master integrals for three-loop four-particle scattering*, *JHEP* **04** (2020) 167, [[2002.09492](#)].
- [16] J. M. Henn, *Multiloop integrals in dimensional regularization made simple*, *Phys. Rev. Lett.* **110** (2013) 251601, [[1304.1806](#)].
- [17] T. Gehrmann and E. Remiddi, *Numerical evaluation of harmonic polylogarithms*, *Comput. Phys. Commun.* **141** (2001) 296–312, [[hep-ph/0107173](#)].
- [18] J. M. Henn, *Lectures on differential equations for Feynman integrals*, *J. Phys. A* **48** (2015) 153001, [[1412.2296](#)].
- [19] S. Badger, C. Brønnum-Hansen, D. Chicherin, T. Gehrmann, H. B. Hartanto, J. Henn et al., *Virtual QCD corrections to gluon-initiated diphoton plus jet production at hadron colliders*, *JHEP* **11** (2021) 083, [[2106.08664](#)].
- [20] S. P. Martin, *Interference of Higgs Diphoton Signal and Background in Production with a Jet at the LHC*, *Phys. Rev. D* **88** (2013) 013004, [[1303.3342](#)].
- [21] L. J. Dixon and Y. Li, *Bounding the Higgs Boson Width Through Interferometry*, *Phys. Rev. Lett.* **111** (2013) 111802, [[1305.3854](#)].
- [22] J. A. M. Vermaseren, *Axodraw*, *Comput. Phys. Commun.* **83** (1994) 45–58.
- [23] D. Binosi and L. Theussl, *JaxoDraw: A Graphical user interface for drawing Feynman diagrams*, *Comput. Phys. Commun.* **161** (2004) 76–86, [[hep-ph/0309015](#)].
- [24] Nicolas Deutschmann, “Qgraf-xml-drawer.”
- [25] Inkscape Project, “Inkscape.”